Rev.Adv.Mater.Sci. 25 (2010) 176-182

# DISTRIBUTION OF MICROHARDNESS AND TENSILE PROPERTIES IN ALUMINUM BILLET PROCESSED BY EQUAL-CHANNEL ANGULAR PRESSING

**K.V. Ivanov and E.V. Naydenkin**

Institute of Strength Physics and Materials Science, Siberian Branch of Russian Academy of Sciences
Academichesky av. 2/4, 634021, Tomsk, Russia

*Received: December 08, 2009*

**Abstract.** The distribution of mechanical properties in a billet of pure aluminum (99.99%) processed by equal-channel angular pressing has been studied using microhardness measurement and tensile testing. It has been found that the variation of microhardness, ultimate strength and elongation up to failure is insignificant for the all studied samples whereas the yield strength of the samples cut from the core of the billet exceeds the respective value obtained for the samples cut from the layers in the vicinity of the top and bottom surfaces by up to 30%. The latter demonstrate essential deformation hardening during plastic flow. In order to explain the difference in deformation behavior, the detailed structural study has been carried out by means of electron-backscattered diffraction analysis.

## 1. INTRODUCTION

Ultrafine-grained metal materials processed by severe plastic deformation are of great interest to material scientists at the recent decade [1,2]. One of the principal ways of severe plastic deformation processing is equal-channel angular pressing (ECAP) which allows one to deform bulk billets preserving their initial shape [3,4]. Due to characteristic features of the structure formed by ECAP, ultrafine-grained materials exhibit unique properties which may be attractive for applications. It is strongly desirable the level of properties and, consequently, parameters of the structure causing the above properties would be the same in the different parts of a billet. It should be noted that investigation of structure is performed in the most of works dealing with the effect of severe plastic deformation processing on the structure and properties of metallic materials. However, detailed description of the structure in the different areas of the same billet processed by equal-channel angular pressing is available in the limited works and distribution of mechanical properties is studied mostly using microhardness measurements. Analysis of literature reveals a discrepancy of experimental data on the homogeneity of structural parameters and mechanical properties in an ECAP-processed billet. On the one hand, using electron-backscattered diffraction (EBSD) analy-

Corresponding author: K.V. Ivanov, e-mail: ikv@ispms.tsc.ru

sis it has been shown in [5] that a homogeneous distribution of structural parameters, namely average subgrain size and fraction of high-angle grain boundaries takes place in the billet of high-purity aluminum as a result of 12 passes of ECAP according the $B_c$ root. It has been found that distribution of microhardness in the billets of high purity aluminum (99.99%) and 6061 aluminum alloy processed by ECAP for 4 and more passes is practically homogeneous [6-8]. The microhardness decreases a little only in the small region nearby the bottom surface of the billet. According to [7], the above result is in a good correspondence with numerical modeling by the finite elements method [9-11]. On the other hand the essential heterogeneous distributions of average grain size (distance between high-angle grain boundaries) and the fraction of high angle grain boundaries with practically homogeneous distribution of average subgrain size and microhardness has been observed in the billet of high-purity aluminum processed by 8 passes of ECAP [12]. A significant scattering of structural parameters and creep characteristics has been found in the samples of pure aluminum processed by 8 and 12 passes of ECAP [13,14].

Taking into account the above, the main task of the present work is to investigate the distribution of microhardness and tensile properties, i.e. ultimate and yield strength, deformation up to failure, shape of flow curves in the billet of ultrafine-grained aluminum processed by ECAP, compare the results with the available literature data on distribution of mechanical properties obtained by microhardness measurements and creep tests and explain peculiarities in the distribution using structure investigation.

## 2. EXPERIMENTAL

The material used in this study was pure aluminum (99.99%). The as-received material was cut to provide a billet with dimensions of 12×12×40 mm$^3$. This billet was previously annealed at 500 °C for 1 hour. Optical microscopy revealed a recrystallized grain size of about 1 mm. The ECAP die channel was of square cross section, with a side of 12 mm. The internal angle ($\Phi$) between the die channels was 90°, and the angle ($\Psi$) subtended by the outer arc of curvature at the intersection between the two channel sections was 37°. For each pass through a die the equivalent strain calculated according to the equation represented in [2,3] was 1. The ECAP processing was performed at room temperature (298K) using a hydraulic press operating at a ram speed of $3.3 \cdot 10^{-1}$ mm/s. The billet was pressed 8 times following route $B_c$ [2,3].

Fig. 1 illustrates the coordinate system state and the scheme of the samples cutting. The flat tensile samples having double-spade shape with the gauge size of 4×2.5×1 mm$^3$ were cut in the longitudinal horizontal section (*xy* plane) by electric-spark method. 10 samples were obtained and five of them were chosen for the investigation. *Z* coordinate corresponding to the distance from the top surface of the billet to the sample position was fixed for the each sample. 3 samples cut from recrystallized aluminum were strained also to evaluate the change of mechanical properties as a result of ECAP.

The structure of each tensile sample was investigated by electron-backscattered diffraction (EBSD) method [15]. One of the flat surfaces of the samples lying in *xy* plane (Fig. 1) was grinded to remove surface layer of approximately 50 μm thick, then mechanically polished with a succession of abrasives which concluded with diamond suspension of 1 μm. Final electropolishing was accomplished at 30 V for 10 to 20 seconds using a 10% $HClO_4$ + 90% $CH_3OH$ solution cooled to -30 °C. Quanta 200 3D scanning electron microscope with tungsten hot cathode operated at 30 kV and work distance of 15 mm was used as an orientation probe during the structural investigation. The size of the scanning area was 30×30 μm and the step size was equal to 0.3 μm. Kikuchi pattern for each point of the scan formed by backscattered electrons was captured by system software (TSL OIM data collection) and then analyzed and indexed. The accuracy of the orientation determination by EBSD method is ~1°

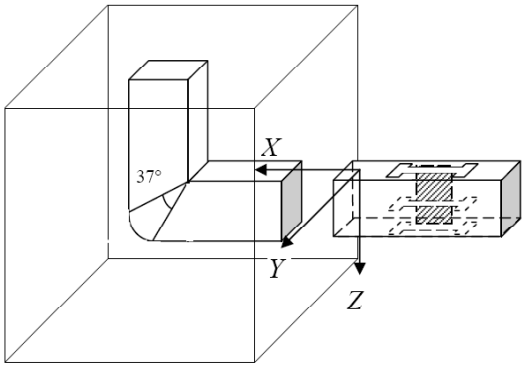


**Fig. 1.** The scheme illustrated the position of the system of coordinates and how the tensile samples and the sample for microhardness measurements were cut. The latter sample is marked by hatching.

**Table 1.** Ultimate strength, yield strength, average grain size and fraction of high-angle grain boundaries obtained for the tested tensile samples.

| Sample number | Distance from the top surface,mm | Ultimate strength, MPa | Yield strength, MPa | Engineering/ true elongation up to failure, % | Number of grains in the EBSD scan | Average grain size, μm | | Fraction of high-angle grain boundaries |
|---|---|---|---|---|---|---|---|---|
| | | | | | | On the each scan | Simple mean of 3 scans | |
| 1 | 2 | 127 | 106 | 32/28 | 212 | 3.9 | 6.7 | 70 |
| | | | | | 157 | 7.2 | | 59 |
| | | | | | 167 | 8.9 | | 60 |
| 2 | 4 | 124 | 120 | 32/28 | 186 | 4.4 | 6.2 | 72 |
| | | | | | 125 | 6.4 | | 62 |
| | | | | | 116 | 7.7 | | 53 |
| 3 | 6 | 132 | 131 | 32/27 | 128 | 7.2 | 5.1 | 57 |
| | | | | | 185 | 4.0 | | 71 |
| | | | | | 184 | 4.0 | | 72 |
| 4 | 8 | 127 | 126 | 31/27 | 168 | 4.7 | 4.4 | 72 |
| | | | | | 203 | 4.1 | | 74 |
| | | | | | - | - | | - |
| 5 | 10 | 123 | 95 | 30/26 | 149 | 6.0 | 12.3 | 67 |
| | | | | | 160 | 4.3 | | 70 |
| | | | | | 54 | 26.6 | | 41 |

[15]. The data obtained were processed using TSL OIM analysis software. The fraction of non-indexed points situated mainly nearby grain boundaries did not exceeds 15%. Individual points having a lower probability of correct automatic indexing were assigned to neighboring regions of similar orientation. It was assumed that grain (subgrain) was a region inside which the disorientation angle between the neighboring points did not exceed the so-called tolerance angle. The tolerance angle was determined to 15 and 2 degrees for grains and subgrains, respectively. The average grain (subgrain) size was defined as a diameter of circle having the same area as the area of the grain (subgrain). The average grain (subgrain) size in the scan area was calculated according to following formula

$$< d >= \frac{\sum_{i=1}^{N} S_i d_i}{\sum_{i=1}^{N} S_i},$$

where $S_i$ and $d_i$ were the square and size of the *i-th* grain, respectively. It should be noted that sometimes scanning area contained only part of grains especially for large grains so the measured average grain size was only a lower limit of the value. Each sample was scanned three times. The scanning areas were chosen occasionally on the gauge. OIM (orientation imaging microscopy) color-coded map, average grain and subgrain size, distribution of boundaries on misorientation angle were obtained for every scanning. Experimental data were summarized in Table 1. Deformation relief arisen on the preliminary polished surface of the tensile samples was studied using Zeiss EVO-50 scanning electron microscope with $LaB_6$ hot cathode operated at 20 kV.

The profile of Vickers microhardness was measured on the sample cut in the longitudinal vertical section nearby the gauge of tensile samples (*xz* plane in Fig. 1) using Duramin-5 tester at 0.1 N load for 10 s along *z* axis with a spacing between each indentation point of ~0.2 mm. The error of the measurement did not exceed 10%. Tensile testing was carried out using PV 3012 testing machine at room temperature. The “time – load” curves were recorded automatically. The strain rate was $8.6 \cdot 10^{-3}$ $s^{-1}$. Engineering stress $\sigma_e$ and engineering plastic strain $\varepsilon_e$ were converted into the true stress $\sigma_t$ and true plastic strain $\varepsilon_t$ by using the well-known relations, $\sigma_t=\sigma_e(1+\varepsilon_e)$ and $\varepsilon_t=\ln(1+\varepsilon_e)$. The yield strength was taken to be the stress corresponding to plastic strain $\varepsilon_e=0.002$ and the ultimate strength met the maximum true stress on the stress – strain curves.

One of the flat surfaces of the test samples was prepared for structural investigation as described above. The other ones were fine grinded on abrasive paper and then electropolished.

## 3. RESULTS AND DISCUSSION

Microhardness measurement reveals that its value is constant along *z* axis within the method accuracy and is equal on average to 390 MPa. The exceptional case is a region of 0.5 mm thick nearby the billet bottom surface where the microhardness decreases by more than 10% relative to the average value down to 340 MPa. The above result is in a perfect correspondence with the data of [6-8]. Thus it is reasonable to consider the homogeneous distribution of microhardness along *z* in the ECAP processed billet of aluminum except the narrow layer near the bottom. The latter is probably due to the development of a shearing zone instead of a shear plane during ECAP [8].

Fig. 2 represents the true curves of plastic flow obtained for the samples corresponding the different distance from the top surface, i.e. *z* coordinate. The flow curves of the samples cut from the core of the billet (samples 3, 4) demonstrate the following characteristic features. Firstly, high values of ultimate strength and yield strength (125 – 130 MPa). The ultimate and yield strengths of recrystallized aluminum are equal to 58 and 49 MPa respectively. Thus ECAP processing of aluminum allows one to increase the ultimate and yield strengths by 2.2 and 2.6 times respectively. Elongation up to failure remains high enough and is equal to approximately 30% (compare with 60% obtained for recrystallized aluminum). Secondly, it should be noted the practically absence of deformation hardening stage of plastic flow so the yield strength is very close to ultimate strength. The difference between them is less than 1%. The authors of [2,3] suggest that the above feature is related to increase of fraction of high-angle grain boundaries and to a consequent change in the dominant deformation mechanisms due to the increasing tendency for the occurrence of grain boundary sliding and grain rotation. The change of the deformation mechanism of ultrafine-grained aluminum relative to coarse-grained counterpart is found in [16]. The authors of [16] indicate that this mechanism is related to grain boundaries. Investigation of deformation relief on the preliminary polished surface of the sample by SEM is shown that the grain boundary sliding occurs during tension of aluminum at room temperature (Fig. 3a). Black arrows indicate the straight parallel lines inside grains

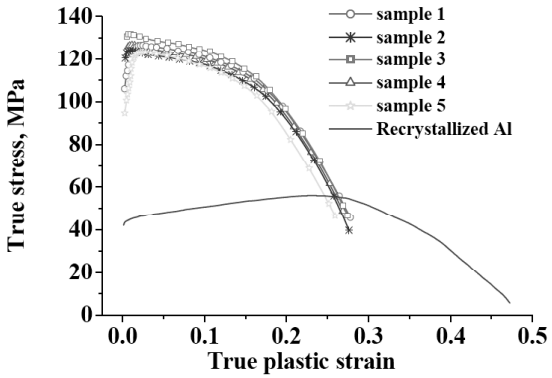


**Fig. 2.** The true plastic flow curves obtained for the test samples corresponding to the different distance from the top surface of the billet. Compare with the flow curve obtained for recrystallized aluminum.

which change direction at grain boundaries. These lines are due to dislocation slip. It should be noted that deformation relief arises on the polished surface of recrystallized aluminum sample but taking into account the straight-line character and the scale factor in the image one can conclude that the relief is related to dislocation slip (Fig. 3b). Thirdly, the characteristic feature of the tension of the samples is very high level of deformation localization. In other words, the strain between yield strength and ultimate strength is rather low (~0.5%).

The flow curves obtained for the samples cut from the layers in the vicinity of the top and bottom surfaces of the billet (samples 1 and 5) appear similar to the discussed above curves of the samples 3 and 4 at the strain higher than that corresponding to ultimate strength. The ultimate strength and elongation up to failure remain practically unchanged. It means that the regularities of strain localization are the same for the all test samples. The very important difference is the presence of short (by strain) stage of strain hardening. The value of the hardening is essential. The difference between the ultimate and yield strength for samples 1 and 5 is 20 to 30%. The flow behavior of the sample 2 is intermediate between the samples 3, 4, and 1, 5.

Undoubtedly, the above difference in the mechanical behavior of the samples is due to the differences in the structure. The structural investigation of the samples prior to deformation revealed the same average subgrain size in the all samples which was equal to 2.2 mm (Fig. 4). This value exactly corresponds to the average subgrain size measured in the central area of *xz* section of the billet [12]. The qualitatively same result was reported in [5], where the OIM maps of subgrain structure

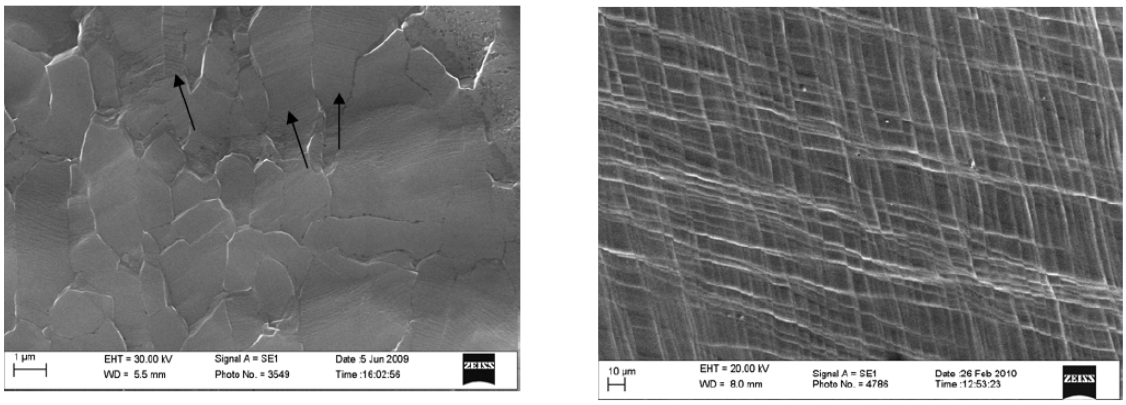


**Fig. 3.** SEM images of deformation relief on the polished surface of the sample 3 at the origin of the neck (a) and that of the recrystallized aluminum sample (b). The sliding between grains and intragrain dislocation slip steps are visible in (a). Black arrows indicate glide lines.

obtained for the different areas of the *xz* section of an ECAP-processed aluminum billet (4 and 12 passes according $B_c$ route) were represented. The difference in the numerical value of average subgrain size measured in the present work and in [5] may be probably attributed to the different way of calculation and, a lesser degree, to different number of ECAP passes. In the cited work the average subgrain size was 1.2 and 1.0 for billets processed for 4 and 12 passes respectively.

The average grain size (the average distance between high-angle grain boundaries) in the samples 2, 3 and 4 cut from the core of the billet varies insignificantly from 4.4 μm for the sample 4 to 6.2 μm for the sample 2. It should be noted the more or less homogeneous distribution of average grain size in the different scans of the samples (Table 1).

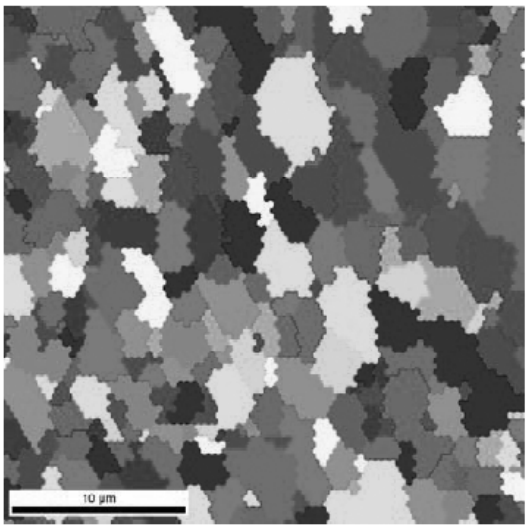


**Fig. 4.** OIM map of subgrain structure obtained for the scan 3 on the sample 5. The same scan as in Fig. 5b.

Sample 5 shows significant growth of the average grain size up to 12.3 μm. This is in a good correspondence with [12] where the similar grain size is reported for the same area of the billet. It should be noted the essential scattering of the average grain size in the sample 5. The limited average grain size of 4.3 and 6.0 μm is obtained in two OIM scans of the sample (Fig. 5a). But the third OIM scan reveals very large average grain size of 26.6 μm (Fig. 5b). The noticeable scatter of the average grain size obtained in different OIM scans of the sample 1 is observed (8.9, 7.2 and 3.9 μm). Despite the average grain size in sample 1 is much less than in the sample 5 and only slightly exceeds the average grain sizes of the samples 2, 3 and 4, its deformation behavior is similar to the sample 5. Study of the deformation relief of the samples 1 and 5 demonstrates grain boundary sliding development during tension. Analyzing the above data one can assume that the samples 1 and 5 exhibit deformation hardening stage during tension due to the presence of regions in the samples where the distance between high-angle grain boundaries is long. In other words, a large grain size corresponds to these areas. The above assumption is suggested by the authors of [14]. They indicate the local structural heterogeneity (inside one sample) as a main reason for the variable time to fracture under creep of samples of ECAP-processed aluminum.

The possible reasons for local structural heterogeneity inside the samples in the vicinity of the top and bottom surfaces and, consequently, for the het-

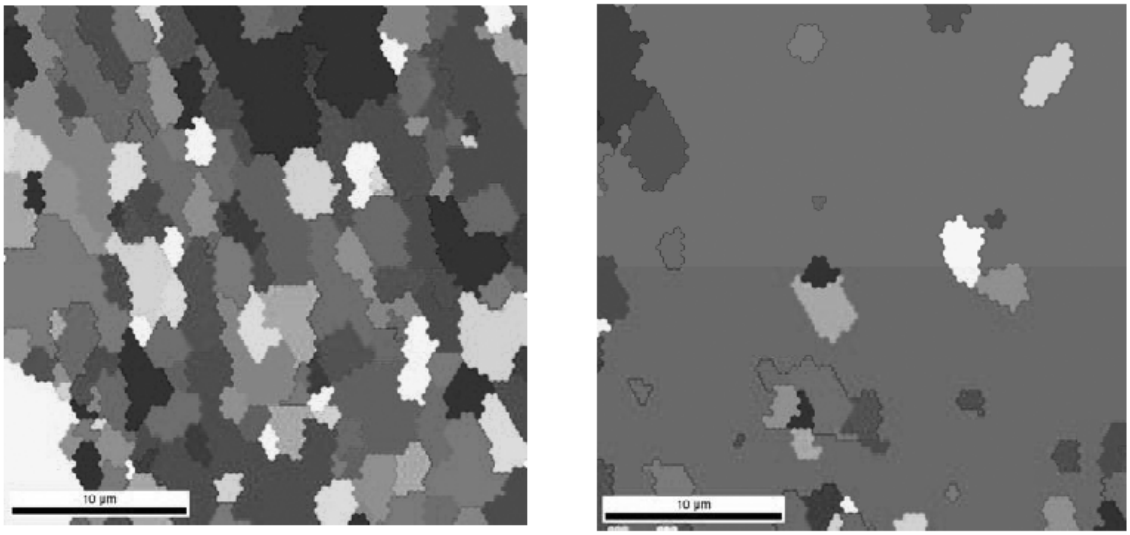


**Fig. 5.** OIM maps of grain structure obtained on the sample 5 for the scans 2 (a) and 3 (b). Compare Figs. 5b and 4 representing the difference of grain and subgrain structure on the same scan.

erogeneity of the total billet processed by ECAP are discussed elsewhere [12]. The most probable origin for the heterogeneity is suggested to be the heterogeneity of plastic shear during ECAP especially in the dies with increased outer angle $\Psi$ (37° in the present work).

## 4. SUMMARY

1. It has been found that the distribution of microhardness, ultimate tensile strength and elongation up to failure is homogeneous along the direction from top to bottom surfaces of the aluminum billet processed by equal-channel angular pressing. However, the yield strength under tension of the core layers of the billet exceeds the respective one obtained for layers in the vicinity of the top and bottom surface by up to 30%.
2. The samples cut from the core layers of the billet exhibit poor deformation hardening under plastic tension. The deformation hardening is much more expressed for the samples corresponding to layers in the vicinity of the top and bottom surface.
3. It is assumed that the heterogeneity of yield strength and the difference in strain behavior is due to local structural heterogeneity in the samples corresponding to the layers in the vicinity of the top and bottom surface of the billet.

The present work has been carried out in the frameworks of the project No. 3.6.2.2 of Siberian Branch of Russian Academy of Sciences.

## REFERENCES

[1] Yu.R. Kolobov, R.Z. Valiev and G.P. Grabovetskaya*, Grain Boundary Diffusion and Properties of Nanostructured Materials* (Cambridge International Science Publishing, Cambridge, 2007).
[2] R.Z. Valiev and I.V. Alexandrov, *Bulk Nanostructured Metallic Materials* (Akademkniga, Moscow, 2007), In Russian.
[3] R.Z.Valiev and T. G. Langdon // *Progr. Mat. Sci.* **51** (2006) 881.
[4] V.M. Segal, V.I. Reznikov, A.E. Drobyshevsky and V.I. Kopylov // *Izvestiya AN SSSR. Metally* **1** (1981) 115, In Russian.
[5] S.D. Terhune, D.L Swisher and K. Oh-Ishi // *Met. Mater. Trans. A.* **33A** (2002) 2173.
[6] M. Prell, Ch. Xu and T. G. Langdon // *Mat. Sci. Eng. A*. **480** (2008) 449.
[7] Ch. Xu and T. G. Langdon // *Scripta Mat*. **48** (2003) 1.
[8] Ch. Xu, M. Furukawa, Z. Horita and T. G. Langdon // *Mat. Sci. Eng. A.* **398** (2005) 66.
[9] V.S. Zhernakov, I.N. Budilov and G.I. Raab // *Scripta Mat.* **44** (2001) 1765.
[10] H.S. Kim // *Mat. Sci. Eng. A*. **328** (2002) 317.
[11] H.S. Kim // *Mat. Sci. Eng. A*. **291** (2000) 86.
[12] K.V. Ivanov and E.V. Naidenkin // *Russian Physics Journal* **52** (2009) 1030.
[13] V. Sklenicka, P. Kral and L. Ilucova // *Mat. Sci. Forum.* **503–504** (2006) 245.

[14] I. Saxl, V. Sklenicka and L. Ilucova // *Mat. Sci. Eng. A*. **503** (2009) 82.
[15] F.J. Humphreys // *J. Mater. Sci.* **36** (2001) 3833.
[16] J. May, H.W. Höppel and M. Göken // *Scripta Mat.* **53** (2005) 189.